Journal of Pain Research

Dovepress
Taylor & Francis Group

Open Access Full Text Article

ORIGINAL RESEARCH

Development and External Validation of a Nomogram for Predicting Postherpetic Neuralgia Risk in Patients with Herpes Zoster: A Retrospective Cohort Study

Lulu Yan[1], Renyuan Deng[2], Hongguang Lu[1], Xiaoping Shen[1]

[1]Department of Dermatology, Affiliated Hospital of Guizhou Medical University, Guiyang, Guizhou, People's Republic of China; [2]Department of Dermatology, People's Hospital of Qiannan Prefecture, Qiannan, Guizhou, People's Republic of China

Correspondence: Hongguang Lu; Xiaoping Shen, Department of Dermatology, Affiliated Hospital of Guizhou Medical University, Guiyang, Guizhou, People's Republic of China, Email hongguanglu@hotmail.com; xiaopingpf@163.com

Background: Postherpetic neuralgia (PHN) is a common and often debilitating complication of herpes zoster (HZ), particularly among older adults and immunocompromised individuals. Characterized by persistent neuropathic pain, PHN is associated with substantial impairment in quality of life and increased healthcare burden. Early identification of patients at high risk for PHN remains challenging in clinical practice.

Methods: This retrospective cohort study included 516 patients with acute HZ from the Affiliated Hospital of Guizhou Medical University between October 2018 and September 2021. Patients were randomly divided into a development cohort (n=362) and an internal validation cohort (n=154), while an independent external validation cohort (n=200) was obtained from another tertiary center. Candidate variables were evaluated using univariable analysis and multivariable logistic regression with backward stepwise selection. A nomogram was developed based on the final model. Model performance was assessed using AUC, calibration plots with Spiegelhalter's Z-test, DCA, and CIC.

Results: PHN occurred in 28.7% of patients in the development cohort. Five predictors were retained in the final model. The nomogram demonstrated acceptable discrimination, with AUCs of 0.758 (95% CI: 0.701–0.815) and 0.746 (95% CI: 0.652-0.841) in the development and external validation cohorts, respectively. Calibration analysis demonstrated satisfactory agreement between predicted and observed outcomes (p=0.761 and p=0.933, respectively). DCA demonstrated a net clinical benefit across threshold probabilities ranging from 18% to 80%, while CIC analysis demonstrated reasonable agreement between predicted high-risk individuals and observed PHN cases across clinically relevant threshold probabilities.

Conclusion: A nomogram for predicting PHN risk was developed and externally validated using readily available clinical variables. The model demonstrated acceptable discrimination, satisfactory calibration, and potential clinical utility, which may support early risk stratification in patients with HZ.

Keywords: postherpetic neuralgia, herpes zoster, nomogram, prediction model, external validation, risk factors

Introduction

Postherpetic neuralgia (PHN), the most common and functionally debilitating complication of herpes zoster (HZ), is characterized by persistent neuropathic pain after resolution of the acute rash.[1,2] After primary infection (varicella), VZV establishes lifelong latency in sensory ganglia, particularly dorsal root ganglia. Declining cell-mediated immunity due to aging, stress, or immunosuppression can trigger viral reactivation, leading to HZ and potentially PHN. Clinically, PHN is commonly defined as pain persisting beyond 90 days after rash onset.[3] Epidemiological studies indicate that approximately 10–30% of patients with HZ develop PHN, with incidence increasing substantially with age, reaching up to 50% in individuals aged ≥60 years and exceeding 70% in those aged >70 years.[4] This demographic trend is of growing

https://doi.org/10.2147/JPR.S617660
Received: 17 April 2026
Accepted: 9 July 2026
Published: 21 July 2026

concern in the context of global population aging. PHN is frequently associated with refractory sleep disturbances, anxiety, depression, and social isolation, resulting in markedly impaired health-related quality of life (HRQoL), increased healthcare utilization, and substantial economic burden.[5]

Despite advances in antiviral and analgesic therapies, PHN often remains difficult to manage once established, highlighting the importance of early risk identification and preventive intervention.[6,7] Several risk factors, including advanced age, severe acute pain, and rash characteristics, have been consistently associated with PHN development.[8,9] Various prediction models for PHN risk assessment have recently been reported, including nomogram-based and machine learning–based approaches.[10–12] However, many existing models were developed using single-center retrospective datasets, lacked independent external validation, or relied on variables that are not routinely available in clinical practice.[13] In contrast, the present study incorporated readily obtainable clinical and laboratory variables and further evaluated model performance in an independent external validation cohort, thereby improving its potential generalizability and clinical applicability.[14,15]

Nomograms have emerged as practical tools for individualized risk prediction by translating multivariable statistical models into intuitive graphical interfaces that facilitate clinical decision-making. Compared with traditional regression equations or complex machine learning approaches, nomograms may offer advantages in interpretability and ease of application, particularly in primary care and resource-limited settings where specialized computational tools are less accessible.[16] Therefore, developing a practical and externally validated prediction model based on routinely available clinical variables may help improve early risk stratification in patients with HZ.

This study aimed to develop and externally validate a nomogram for individualized prediction of PHN risk using readily obtainable clinical and laboratory variables. The model incorporated predictors identified through a structured variable selection process, including age, HZ clinical classification, acute-phase pain intensity, monocyte count, and history of malignant tumor. Model performance was evaluated in terms of discrimination, calibration, and clinical utility using both internal and external validation strategies.

Materials and Methods

Study Population and Data Collection

Patients diagnosed with acute HZ were retrospectively screened from the electronic medical records of the Affiliated Hospital of Guizhou Medical University between October 1, 2018, and September 30, 2021. Cases were identified using the keywords "shingles," "zoster," and "herpes zoster." Among 615 initially screened patients, 516 were included in the final analysis after applying the predefined eligibility criteria (Figure 1). The majority of excluded patients were lost to follow-up before the 3-month assessment and therefore could not be reliably evaluated for PHN outcomes. Patients were randomly divided into a development cohort and an internal validation cohort at a 7:3 ratio. For external validation, an independent cohort of 200 patients with HZ was retrospectively enrolled from the Department of Dermatology at the People's Hospital of Qiannan Prefecture between March 1, 2020, and September 1, 2021.

The inclusion criteria were: (1) a primary hospital discharge diagnosis of HZ; (2) availability of documented pain assessment at baseline and at the 3-month follow-up; and (3) complete baseline clinical and laboratory information required for model development. PHN was defined as neuropathic pain with a Numeric Rating Scale (NRS) score $\geq$3 persisting for at least 3 months after the onset of the acute HZ rash. Exclusion criteria included: (1) incomplete medical records or loss to follow-up before the 3-month assessment; (2) pre-existing chronic pain conditions; and (3) severe cognitive impairment that could compromise the reliability of pain assessments. Patients with missing baseline clinical variables, laboratory data, or unavailable follow-up assessments were excluded before model development. Therefore, a complete-case analysis was performed without multiple imputation.

The following clinicopathological variables were extracted from the medical records: demographic characteristics (age, gender); clinical presentation (acute-phase NRS-11 score and HZ clinical classification, including abortive, common, bullous, hemorrhagic, or generalized forms); and comorbidities (respiratory diseases, coronary heart disease, steatotic liver disease, chronic kidney disease, thyroid disease, diabetes, malignant tumor, HIV). These comorbidities were selected a priori based on previously reported associations with HZ severity or PHN risk, such as malignancy-related immunosuppression, chronic inflammatory conditions, and metabolic disorders. Additional variables included

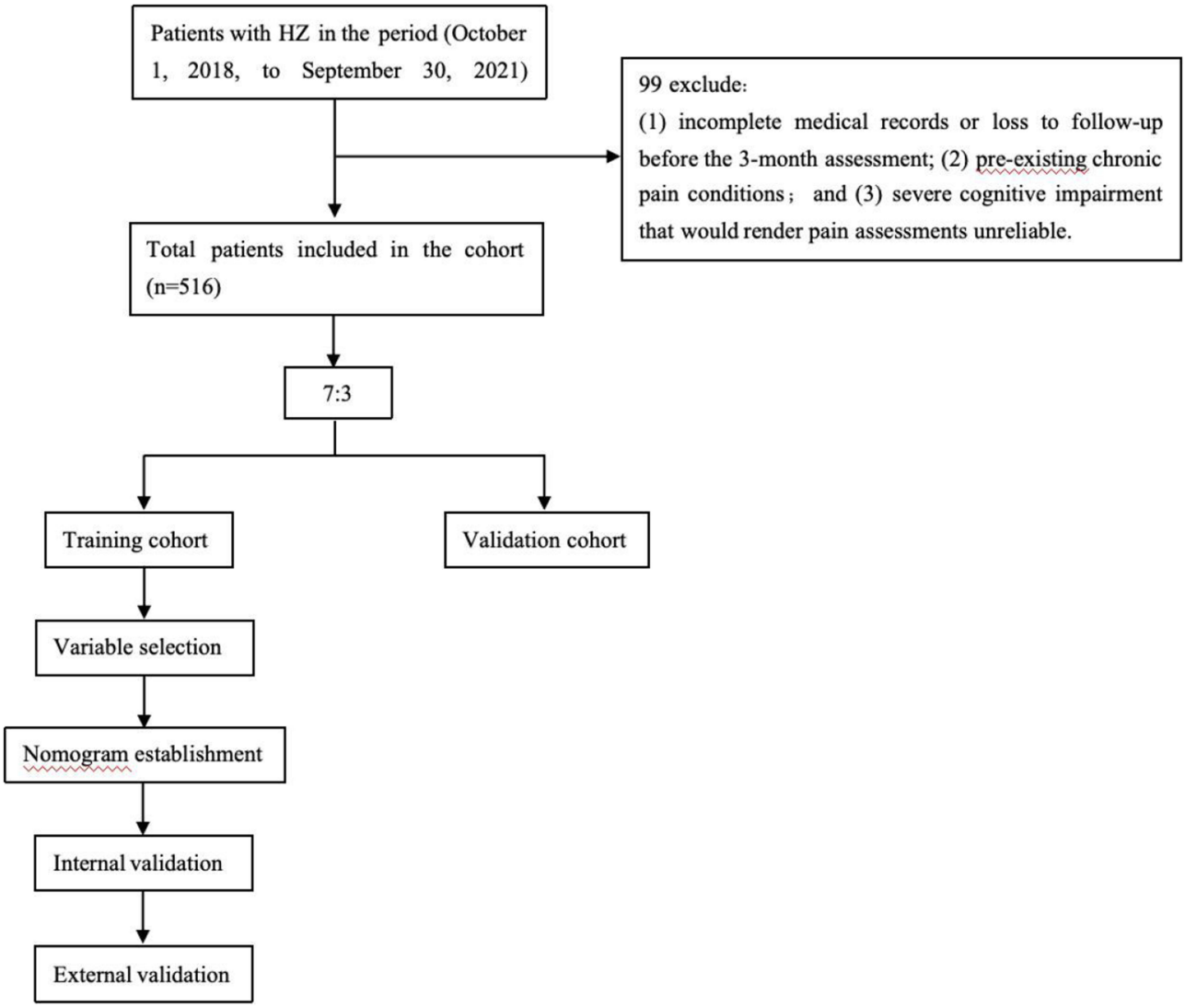

Figure 1 Flowchart of patient selection, cohort allocation, nomogram development, and validation.

lifestyle factors (smoking history, alcohol history), specific treatments (systemic corticosteroid therapy), and laboratory parameters (leukocyte [WBC], lymphocyte [LYMPH], neutrophil [NEUT], and monocyte [MONO] counts). Laboratory parameters were obtained from peripheral blood samples collected during the acute phase of HZ at the time of initial hospital evaluation before initiation of systemic treatment. Pain intensity was rated by patients on the 11-point NRS, where 0 indicates no pain, 1–3 mild pain, 4–6 moderate pain, and 7–10 severe pain. HZ clinical classification was determined according to the predominant cutaneous manifestations documented in the medical records. Bullous and hemorrhagic forms were considered indicative of more severe local inflammatory involvement, whereas generalized HZ referred to disseminated cutaneous lesions extending beyond the primary dermatomal distribution. Abortive HZ referred to zoster-associated pain with absent or minimal cutaneous eruption, whereas common HZ referred to the typical vesicular eruption confined to a dermatomal distribution.

This study was approved by the Ethics Committee of the Affiliated Hospital of Guizhou Medical University (Approval No. 202667), which served as the primary study center. The external validation cohort consisted of retrospectively collected, fully anonymized data without identifiable personal information. The requirement for written informed consent was waived due to the retrospective nature of the study. All procedures were conducted in accordance with the Declaration of Helsinki.

Statistical Analysis

Continuous variables are presented as mean ± standard deviation or median (interquartile range), as appropriate, and were compared using the Student's *t*-test or Mann–Whitney *U*-test. Categorical variables are expressed as numbers (percentages) and were compared using the Chi-square test or Fisher's exact test, as appropriate.

A backward stepwise selection approach was applied to derive a parsimonious multivariable model. Based on the final multivariable model, a nomogram was developed for individualized PHN risk prediction. Model performance was evaluated in terms of discrimination, calibration, and clinical utility. Discrimination was assessed using the area under the receiver operating characteristic curve (AUC). Calibration was evaluated using calibration plots and Spiegelhalter's Z-test. Clinical utility was assessed using decision curve analysis (DCA) and clinical impact curve (CIC) analysis. Internal validation was performed using bootstrap resampling with 1,000 iterations to estimate optimism-corrected model performance.

All statistical analyses were performed using R software (version 4.3.2). A two-tailed p-value <0.05 was considered statistically significant, except for candidate variable selection, where a threshold of p<0.1 in univariate analysis was applied. The conventional two-sided significance level of 0.05 was adopted to balance Type I and Type II error rates, as a more stringent threshold (eg, 0.01) could increase the risk of failing to identify potentially relevant predictors given the sample size. This approach is consistent with standard practice in clinical prediction model research.

Results

Baseline Characteristics

After screening 615 patients, 516 met the eligibility criteria and were included in the final analysis (Figure 1). Among the included patients, 148 (28.7%) developed PHN. The baseline characteristics of the study population stratified by PHN status are summarized in Table 1. All patients had received antiviral therapy before the baseline assessment.

Table 1 Baseline Characteristics of the Study Population Stratified by Postherpetic Neuralgia Status

Variables	Overall	Non-PHN Group (n = 368)	PHN Group (n = 148)	P value
Age, Median (Q1,Q3)	63 (50, 73)	61 (47, 72)	66 (57.75, 73)	< 0.001
Gender				0.589
Men	245 (47.48)	178 (48.37)	67 (45.27)	
Women	271 (52.52)	190 (51.63)	81 (54.73)	
Types of HZ				0.015
Abortive	51 (9.88)	44 (11.96)	7 (4.73)	
Common	366 (70.93)	256 (69.57)	110 (74.32)	
Bullous	47 (9.11)	28 (7.61)	19 (12.84)	
Blood blisters	42 (8.14)	34 (9.24)	8 (5.41)	
Extensive	10 (1.94)	6 (1.63)	4 (2.7)	
Diabetes, n (%)				0.997
No	441 (85.47)	314 (85.33)	127 (85.81)	
Yes	75 (14.53)	54 (14.67)	21 (14.19)	
Chronic lung disease, n (%)				0.18
No	478 (92.64)	345 (93.75)	133 (89.86)	
Yes	38 (7.36)	23 (6.25)	15 (10.14)	
Thyroid disease, n (%)				0.042
No	486 (94.19)	352 (95.65)	134 (90.54)	
Yes	30 (5.81)	16 (4.35)	14 (9.46)	
Cardiovascular disease, n (%)				0.963
No	459 (88.95)	328 (89.13)	131 (88.51)	
Yes	57 (11.05)	40 (10.87)	17 (11.49)	
Steatotic liver disease, n (%)				0.598
No	445 (86.24)	315 (85.6)	130 (87.84)	
Yes	71 (13.76)	53 (14.4)	18 (12.16)	

(*Continued*)

Table 1 (Continued).

Variables	Overall	Non-PHN Group (n = 368)	PHN Group (n = 148)	P value
Chronic kidney disease, n (%)				0.617
No	487 (94.38)	349 (94.84)	138 (93.24)	
Yes	29 (5.62)	19 (5.16)	10 (6.76)	
Malignant tumor, n (%)				0.087
No	500 (96.9)	360 (97.83)	140 (94.59)	
Yes	16 (3.1)	8 (2.17)	8 (5.41)	
HIV, n (%)				0.695
No	508 (98.45)	363 (98.64)	145 (97.97)	
Yes	8 (1.55)	5 (1.36)	3 (2.03)	
Acute phase NRS-11 Score				< 0.001
0 point	8 (1.55)	7 (1.9)	1 (0.68)	
1~3 points (mild)	158 (30.62)	141 (38.32)	17 (11.49)	
4~6points (moderate)	197 (38.18)	149 (40.49)	48 (32.43)	
≥ 7 points (severe)	153 (29.65)	71 (19.29)	82 (55.41)	
Smoking history, n (%)				1
No	424 (82.17)	302 (82.07)	122 (82.43)	
Yes	92 (17.83)	66 (17.93)	26 (17.57)	
Drinking history, n (%)				0.996
No	434 (84.11)	309 (83.97)	125 (84.46)	
Yes	82 (15.89)	59 (16.03)	23 (15.54)	
Hormone therapy				0.547
No	350 (67.83)	253 (68.75)	97 (65.54)	
Yes	166 (32.17)	115 (31.25)	51 (34.46)	
WBC, Median (Q1,Q3)	5.56 (4.51, 6.97)	5.56 (4.58, 6.81)	5.5 (4.35, 7.18)	0.927
NEUT, Median (Q1,Q3)	3.2 (2.45, 4.43)	3.16 (2.45, 4.38)	3.35 (2.45, 4.61)	0.437
LYMPH, Median (Q1,Q3)	1.51 (1.12, 1.96)	1.52 (1.15, 2.06)	1.42 (1, 1.83)	0.025
MONO, Median (Q1,Q3)	0.52 (0.4, 0.66)	0.51 (0.39, 0.64)	0.53 (0.44, 0.69)	0.026

Identification of Independent Predictors and Nomogram Construction

Univariate logistic regression analysis identified several variables associated with PHN risk. Variables with $p<0.1$ in the univariate analysis were subsequently entered into the multivariable logistic regression model. Using a backward stepwise selection approach, five variables were retained in the final model: age, HZ clinical classification, higher acute-phase NRS score, elevated absolute monocyte count (the normal reference range for peripheral blood monocyte count in our institution is 0.1–0.6 $\times 10^9$/L), and history of malignant tumor (Table 2). A nomogram was subsequently developed based on the final multivariable model for individualized PHN risk prediction (Figure 2).

Table 2 Univariate and Multivariable Logistic Regression Analyses for Predictors of Postherpetic Neuralgia

Variables	Univariate Analysis OR (95% CI)	P value	Multivariate Analysis OR (95% CI)	P value
Age	1.02 (1.01–1.04)	<0.001	1.015(0.999~1.032)	0.07
Gender	1.13 (0.77–1.66)	0.524		
Types of HZ	4.27 (1.59–11.45)	0.004	2.764(0.716~10.508)	0.132
Diabetes	0.96 (0.56–1.66)	0.888		
Chronic lung disease	1.69 (0.86–3.34)	0.13		
Thyroid disease	2.30 (1.09–4.84)	0.028		
Cardiovascular disease	1.06 (0.58–1.94)	0.84		
Steatotic liver disease	0.82 (0.46–1.46)	0.505		

(*Continued*)

https://doi.org/10.2147/JPR.S617660

Table 2 (Continued).

Variables	Univariate Analysis OR (95% CI)	P value	Multivariate Analysis OR (95% CI)	P value
Chronic kidney disease	1.33 (0.60–2.93)	0.478		
Malignant tumor	2.57 (0.95–6.98)	0.064	1.716(0.401~7.361)	0.458
HIV	1.50 (0.35–6.37)	0.581		
Acute phase NRS-11 Score	8.08 (0.97–67.30)	0.053	4.301(1.189~32.045)	0.055
Smoking history	0.98 (0.59–1.61)	0.921		
Drinking history	0.96 (0.57–1.63)	0.89		
Hormone therapy	1.16 (0.77–1.73)	0.48		
WBC	1.01 (0.91–1.12)	0.892		
NEUT	1.06 (0.94–1.19)	0.324		
LYMPH	0.70 (0.52–0.94)	0.019		
MONO	3.09 (1.29–7.41)	0.011	2.57(0.815~8.223)	0.107

Model Performance in the Development and Internal Validation Cohorts

The nomogram demonstrated acceptable discrimination in the development cohort, with an AUC of 0.758 (95% CI: 0.701–0.815) (Figure 3A). Similar discriminative performance was observed in the internal validation cohort (Figure 3B).

Calibration analysis demonstrated satisfactory agreement between predicted and observed probabilities in both the development and internal validation cohorts. Spiegelhalter's Z-test showed no significant lack of fit (p=0.761 for the development cohort), and the calibration plots further supported good calibration performance (Figure 4A and B).

Decision curve analysis demonstrated a positive net clinical benefit across a wide range of clinically relevant threshold probabilities in both cohorts (Figure 5A and B). In addition, clinical impact curve analysis showed reasonable agreement between predicted high-risk patients and observed PHN cases, supporting the clinical applicability of the nomogram (Figure 6A and B).

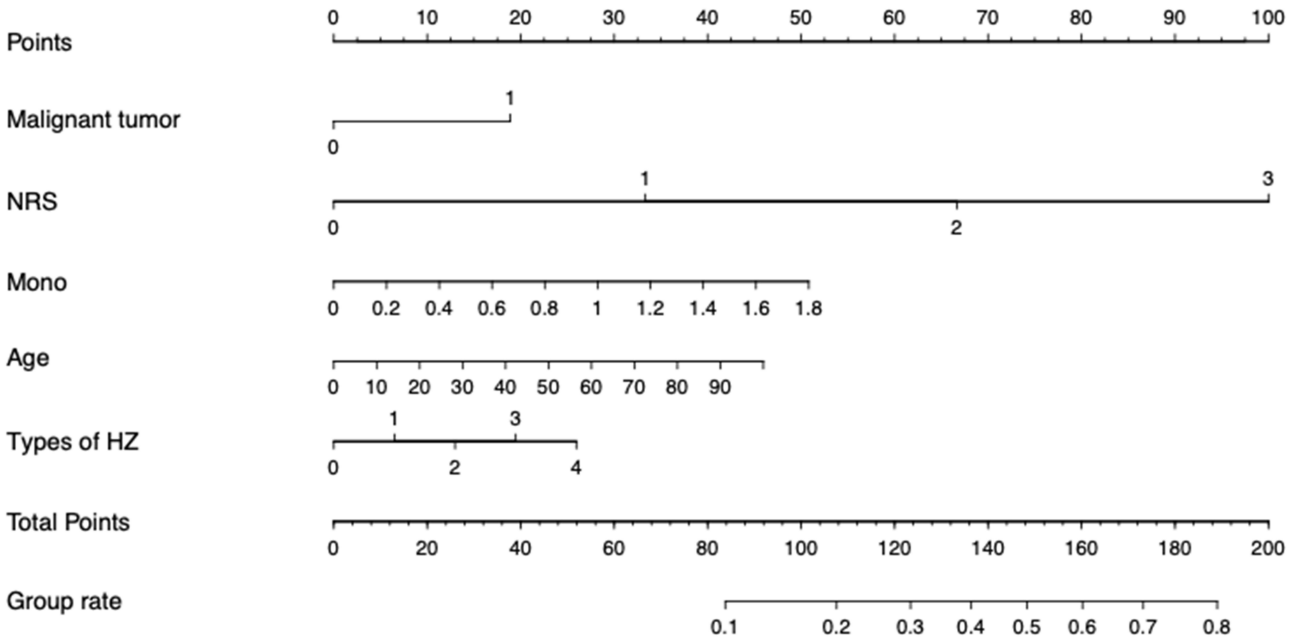

Figure 2 Nomogram for predicting the risk of postherpetic neuralgia (PHN). For acute-phase pain intensity (NRS category): 0 = no pain, 1 = mild pain (NRS 1–3), 2 = moderate pain (NRS 4–6), and 3 = severe pain (NRS 7–10). For herpes zoster (HZ) clinical classification: 0 = abortive, 1 = common, 2 = bullous, 3 = hemorrhagic, and 4 = generalized HZ.

https://doi.org/10.2147/JPR.S617660

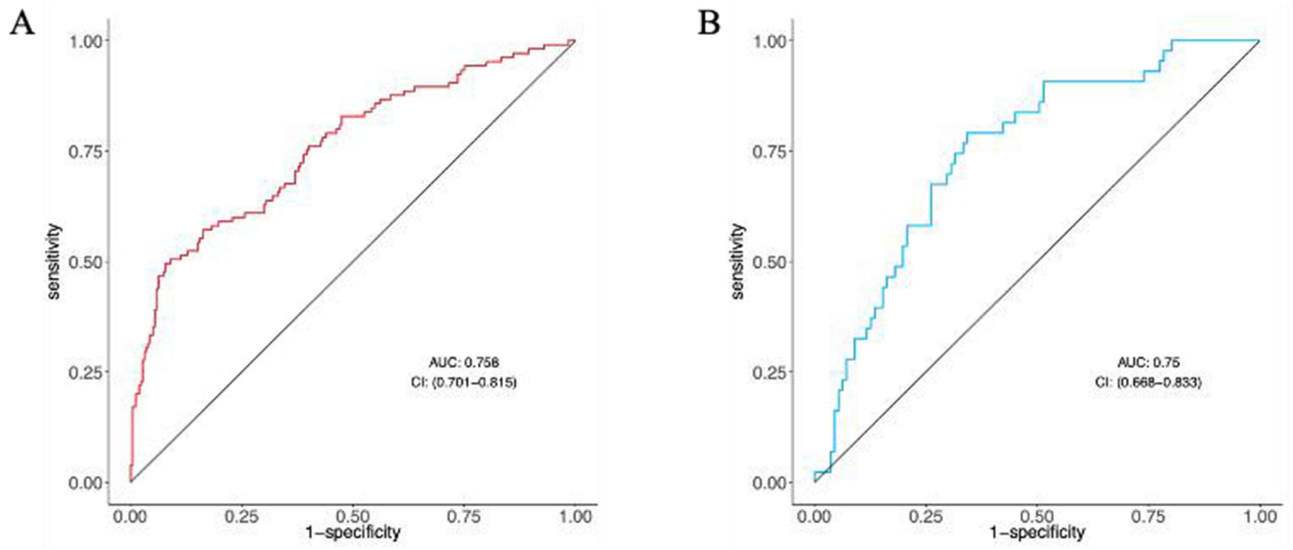

Figure 3 Receiver operating characteristic (ROC) curves showing the discriminative ability of the predictive model (**A**) and the internal validation model (**B**). The colored stepwise curves represent the ROC curves of the corresponding models, illustrating the relationship between sensitivity and 1-specificity across different threshold values. The diagonal straight line represents the reference line for no discriminative ability, corresponding to an area under the curve (AUC) of 0.5. A curve located farther above the diagonal line indicates better model discrimination. The AUC values with corresponding confidence intervals are shown in each panel.

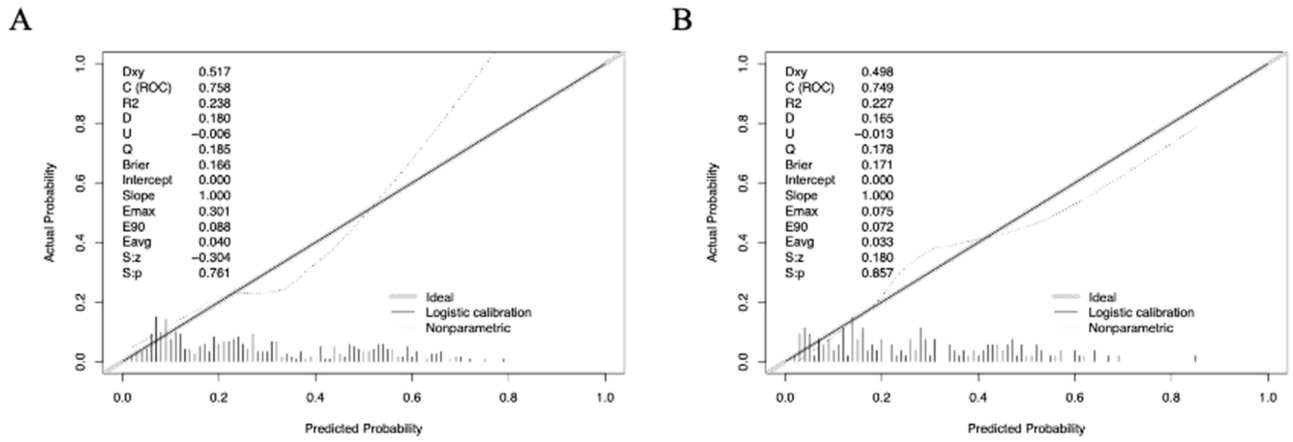

Figure 4 Calibration curves of the predictive model (**A**) and internal validation model (**B**). The diagonal straight line represents the ideal calibration curve, indicating perfect agreement between the predicted and observed probabilities. The solid line represents the logistic calibration curve of the model, while the dotted line represents the nonparametric calibration curve. The shaded/rug area along the x-axis indicates the distribution of predicted probabilities among the study samples. A calibration curve closer to the diagonal straight line suggests better agreement between predicted and actual outcomes.

External Validation

The external validation cohort, comprising 200 patients from an independent center, was used to further assess the generalizability of the model. The nomogram maintained acceptable discrimination in the external validation cohort, with an AUC of 0.746 (95% CI: 0.652-0.841) (Figure 7A).

Calibration analysis demonstrated good agreement between predicted and observed outcomes, as indicated by a non-significant Spiegelhalter's Z-test result (p=0.933) and the corresponding calibration plot (Figure 7B).

Furthermore, decision curve analysis demonstrated a favorable net clinical benefit across clinically relevant threshold probabilities (Figure 7C), while clinical impact curve analysis showed reasonable concordance between predicted high-risk patients and observed PHN cases (Figure 7D), supporting the potential clinical utility of the nomogram in an independent external population.

https://doi.org/10.2147/JPR.S617660

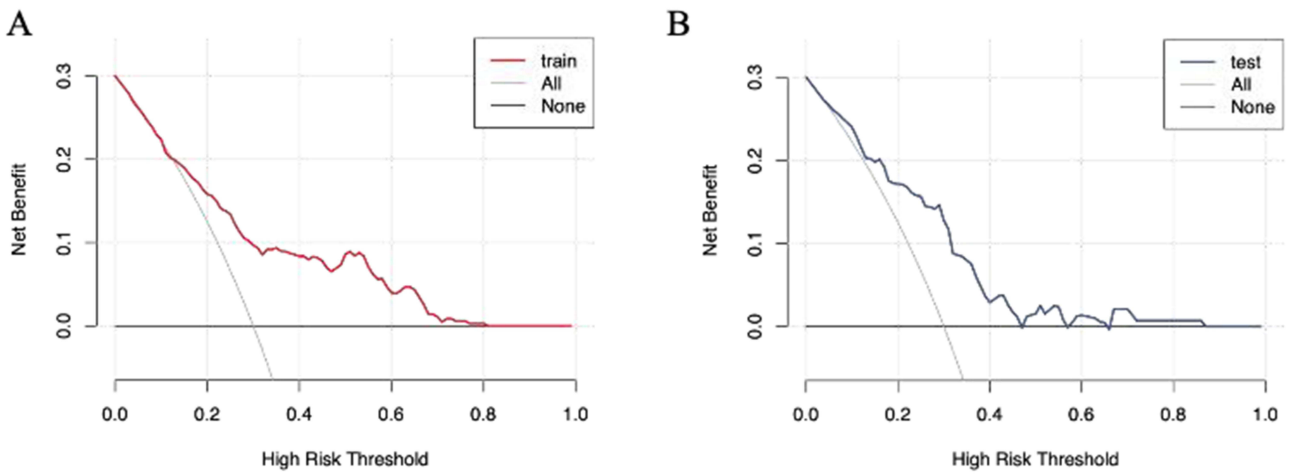

Figure 5 Decision curve analysis (DCA) curves evaluating the clinical utility of the predictive model (**A**) and the internal validation model (**B**). The colored curve represents the net benefit of the corresponding model across different high-risk threshold probabilities. The curved grey line labeled "All" represents the net benefit obtained by assuming that all individuals are high-risk and would receive intervention. The horizontal black line labeled "None" represents the net benefit obtained by assuming that no individuals are high-risk and no intervention is given. A model curve located above both reference lines indicates greater clinical net benefit within the corresponding threshold probability range.

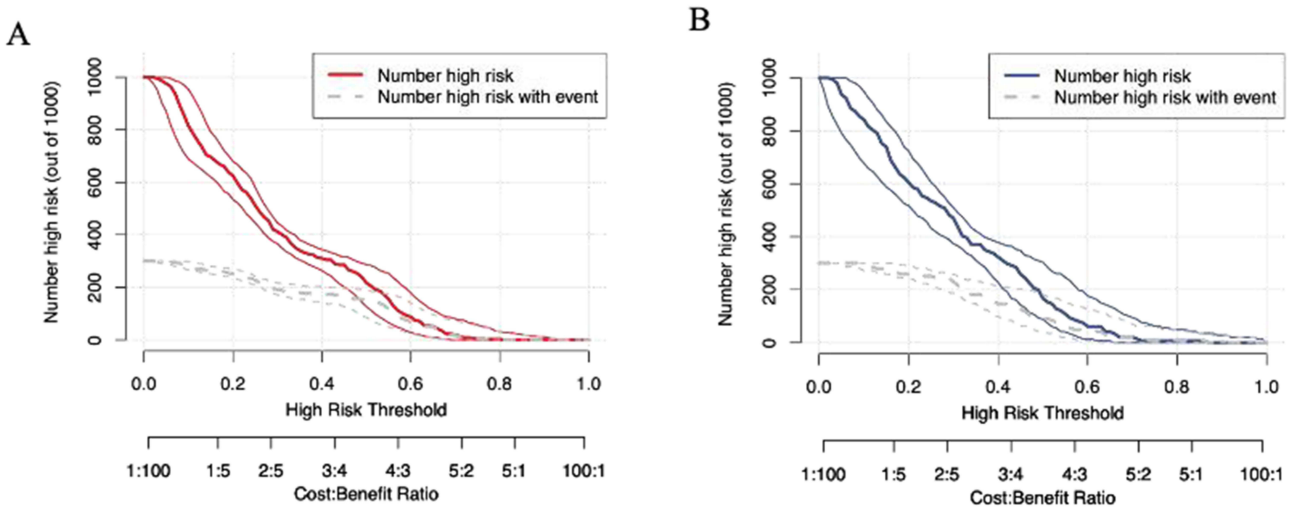

Figure 6 Clinical impact curves of the predictive model (**A**) and the internal validation model (**B**). The red lines in (**A**) and the blue lines in (**B**) represent the estimated number of individuals classified as high risk by the corresponding model across different high-risk threshold probabilities. The grey lines represent the estimated number of high-risk individuals who would actually experience the event. For each color, the middle line indicates the estimated curve, while the upper and lower lines indicate the corresponding confidence interval. The x-axis shows the high-risk threshold probability, with the corresponding cost–benefit ratio displayed below, and the y-axis shows the number of high-risk individuals per 1,000 subjects.

Discussion

In this study, a nomogram for individualized prediction of PHN risk in patients with acute HZ was developed and externally validated using five readily available clinical variables: age, HZ clinical classification, history of malignant tumor, acute-phase NRS score, and monocyte count. The model demonstrated acceptable discrimination, satisfactory calibration, and potential clinical utility in both the development and external validation cohorts, suggesting its potential utility for early risk stratification in clinical practice. Furthermore, the identified predictors are generally consistent with previously reported clinical risk factors for PHN and support the relevance of inflammatory and host-related factors in PHN development.

Among the identified predictors, advanced age emerged as an important factor associated with PHN risk. This finding is consistent with previous studies and may be partially explained by age-related alterations in immune function,

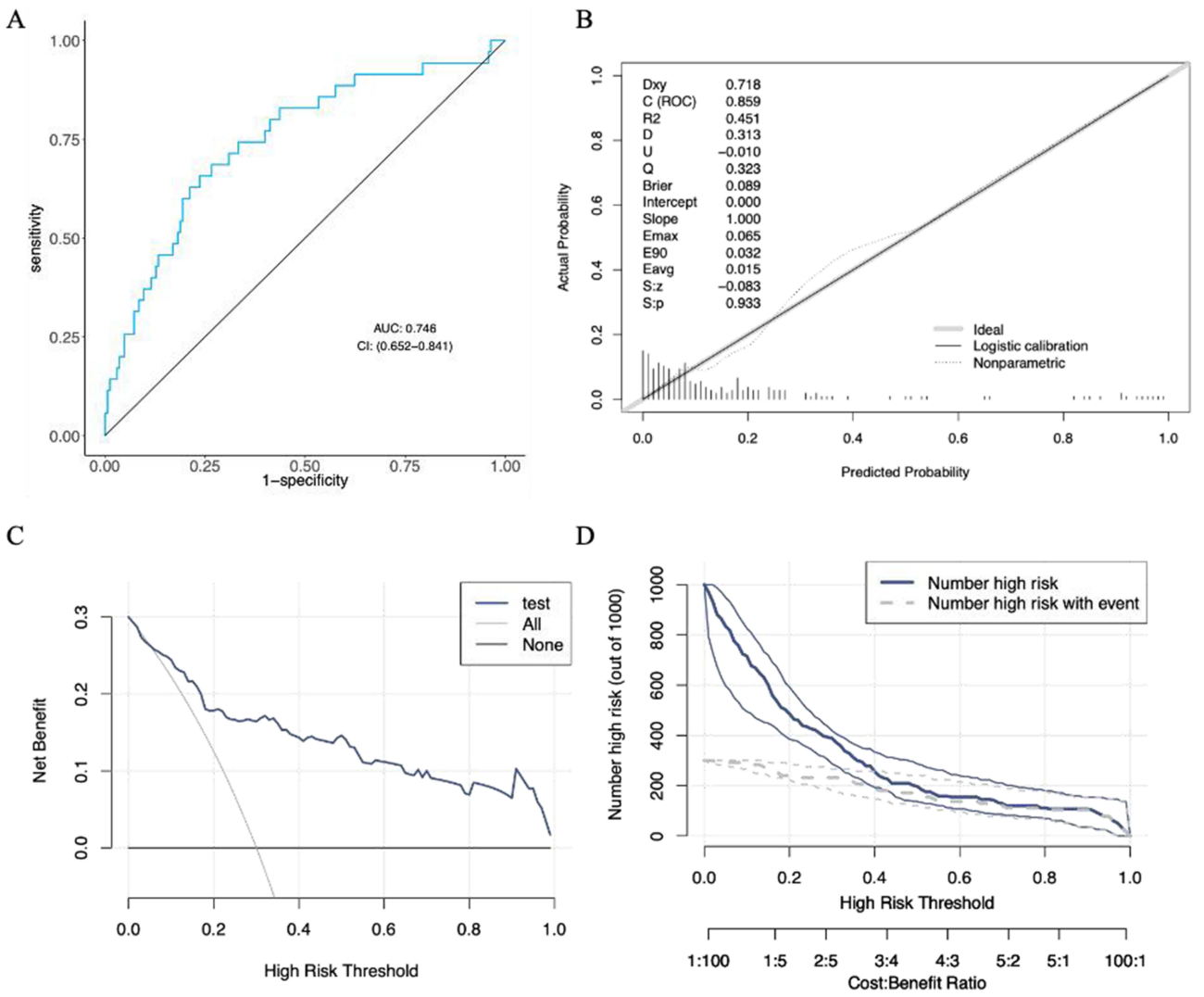

Figure 7 Performance of the nomogram in the external validation cohort. (**A**) Receiver operating characteristic (ROC) curve showing the discriminative ability of the nomogram. The blue curve represents the ROC curve of the model, and the diagonal grey line represents the reference line for no discriminative ability. The area under the curve (AUC) was 0.746. (**B**) Calibration curve showing the agreement between predicted and observed PHN probabilities. The diagonal straight line represents the ideal calibration curve, indicating perfect agreement between predicted and observed probabilities. The solid calibration line represents the model-based logistic calibration curve, while the dotted line represents the nonparametric calibration curve. The rug marks along the x-axis indicate the distribution of predicted probabilities. Spiegelhalter's Z-test showed good calibration performance (P=0.933). (**C**) Decision curve analysis (DCA) evaluating the clinical utility of the nomogram. The blue curve represents the net benefit of the nomogram across different high-risk threshold probabilities. The curved grey line labeled "All" represents the net benefit when all individuals are assumed to be high risk and receive intervention, whereas the horizontal black line labeled "None" represents the net benefit when no individuals receive intervention. (**D**) Clinical impact curve (CIC) assessing the clinical applicability of the nomogram. The solid blue line represents the number of individuals classified as high risk by the model at each threshold probability, and the grey dashed line represents the number of high-risk individuals who actually experienced PHN events. The x-axis shows the high-risk threshold probability, with the corresponding cost–benefit ratio shown below.

commonly referred to as immunosenescence.[17,18] Declining virus-specific cellular immunity in older individuals may impair control of varicella-zoster virus reactivation, thereby contributing to more extensive neural inflammation and delayed recovery following acute HZ.[19] In addition, aging has been associated with impaired neuronal repair capacity and a chronic low-grade inflammatory state, both of which may contribute to persistent neuropathic pain.[20,21] Therefore, age may represent not only a demographic characteristic but also a clinically relevant surrogate marker of impaired antiviral immunity and reduced neural recovery capacity.

This analysis also identified HZ clinical classification as an independent predictor of PHN. Patients presenting with more severe cutaneous manifestations, including bullous, hemorrhagic, or generalized forms of HZ, tended to have a higher risk of developing PHN. These severe clinical phenotypes may reflect more extensive viral involvement and

https://doi.org/10.2147/JPR.S617660

a heightened inflammatory response during the acute phase of infection.[22,23] Previous studies have suggested that inflammatory mediators and tissue injury associated with severe HZ may contribute to peripheral nerve damage and persistent sensitization.[24,25] Accordingly, the severity of cutaneous involvement may serve as a clinically accessible indicator of underlying neural injury and inflammatory burden.

A history of malignant tumor was also independently associated with PHN risk in our cohort. This association may be related to the immunosuppressive effects of malignancy itself or anticancer treatments such as chemotherapy, which can impair antiviral immune responses and delay tissue recovery.[9] Patients with malignancy may therefore be more susceptible to prolonged neural inflammation and persistent neuropathic pain following HZ.

Acute-phase pain intensity, assessed using the NRS, was another important predictor in the present model. Severe acute pain has consistently been associated with subsequent PHN development in previous studies.[6,26] Intense nociceptive stimulation during the acute phase of HZ may contribute to peripheral and central sensitization, thereby increasing the likelihood of persistent pain after rash resolution.[27–30] From a clinical perspective, this finding further supports the importance of adequate early pain management in patients with acute HZ, particularly among individuals presenting with severe pain at baseline.

Therefore, elevated peripheral monocyte counts may reflect an enhanced systemic inflammatory response associated with increased susceptibility to persistent neuropathic pain.[31–33] Monocytes are important mediators of innate immune activation and may contribute to neuroinflammatory signaling through the release of pro-inflammatory cytokines, including TNF-α, IL-1β, and IL-6.[31] Previous studies have also reported associations between alterations in monocyte subsets and chronic pain conditions.[32] In addition, monocytes may differentiate into tissue macrophages that participate in the maintenance of neuroinflammatory responses during chronic neuropathic pain states.[33]

Although the precise biological mechanisms underlying these associations remain unclear, peripheral monocyte count may represent a simple and accessible biomarker for PHN risk assessment.

The nomogram developed in this study integrates these clinical and laboratory variables into an intuitive tool for individualized PHN risk prediction. The model demonstrated acceptable discrimination and satisfactory calibration in both the development and external validation cohorts. In addition, DCA suggested potential clinical utility across a range of clinically relevant threshold probabilities, indicating that the model may assist clinicians in identifying patients at elevated risk for PHN who may benefit from closer monitoring or early preventive management. Because all included predictors are routinely available in standard clinical practice, the nomogram may be feasible for implementation across a variety of clinical settings. Similarly, the CIC findings demonstrated reasonable concordance between predicted high-risk individuals and observed PHN cases, further supporting the potential clinical applicability of the nomogram.

Limitations

Several limitations of this study should be acknowledged. First, this was a retrospective study and may therefore be subject to selection bias and residual confounding. Second, the study population consisted primarily of hospitalized patients from two centers in China, which may limit the generalizability of the findings to other populations or outpatient settings. Third, although external validation was performed, further prospective multicenter validation is still required before broader clinical application. In addition, variable selection was performed using a backward stepwise approach, which may introduce model instability. Finally, dynamic inflammatory biomarkers and longitudinal immune parameters were not evaluated in the present study, and the biological mechanisms underlying the observed associations warrant further investigation.

Conclusion

A nomogram for individualized prediction of PHN risk in patients with acute HZ was developed and externally validated using readily available clinical and laboratory variables. The model demonstrated acceptable discrimination, satisfactory calibration, and potential clinical utility. More severe HZ clinical phenotypes, including bullous, hemorrhagic, and generalized forms, were associated with an increased risk of PHN and may serve as readily identifiable clinical indicators for early risk assessment. This nomogram may serve as a practical tool for early risk stratification and individualized management in patients with HZ. Further prospective multicenter studies are warranted to validate its clinical applicability.

Data Sharing Statement

The datasets generated and/or analyzed during the current study are not publicly available due to institutional restrictions and patient privacy considerations but are available from Professor Xiaoping Shen (Email: xiaopingpf@163.com) upon reasonable request and with permission from the relevant institutional review boards.

Ethics Statement

This study was approved by the Ethics Committee of the Affiliated Hospital of Guizhou Medical University (Approval No. 202667), which served as the primary study center. The external validation cohort consisted of retrospectively collected and fully anonymized data, and no additional ethical approval was required according to institutional policies. The requirement for written informed consent was waived due to the retrospective nature of the study. All procedures were conducted in accordance with the Declaration of Helsinki.

Acknowledgments

The authors thank all patients who participated in this study.

Author Contributions

All authors made a significant contribution to the work reported, whether that is in the conception, study design, execution, acquisition of data, analysis and interpretation, or in all these areas; took part in drafting, revising or critically reviewing the article; gave final approval of the version to be published; have agreed on the journal to which the article has been submitted; and agree to be accountable for all aspects of the work.

Funding

This research received no external funding.

Disclosure

The authors report no conflicts of interest in this work.

References

1. Schmader K. Herpes Zoster. *Ann Intern Med*. 2018;169(3):Itc19–itc31. doi:10.7326/L18-0558
2. Gross GE, Eisert L, Doerr HW, et al. S2k guidelines for the diagnosis and treatment of herpes zoster and postherpetic neuralgia. *J Dtsch Dermatol Ges*. 2020;18(1):55–78.
3. Johnson RW, Rice AS. Clinical practice. Postherpetic neuralgia. *N Engl J Med*. 2014;371(16):1526–1533. doi:10.1056/NEJMcp1403062
4. Matthews S, De Maria A, Passamonti M, et al. The economic burden and impact on quality of life of herpes zoster and postherpetic neuralgia in individuals aged 50 years or older in Italy. *Open Forum Infect Dis*. 2019;6(2):ofz007. doi:10.1093/ofid/ofz007
5. Jiang X, Yan Y, Chen Z, et al. The basolateral amygdala-anterior cingulate cortex circuit contributes to postherpetic neuralgia-anxiety comorbidity. *Theranostics*. 2025;15(10):4614–4637. doi:10.7150/thno.111130
6. Warner DB, Jeng BH, Kim J, et al. Low-dose valacyclovir for postherpetic neuralgia in the zoster eye disease study: a randomized clinical trial. *JAMA Ophthalmol*. 2025;143(4):277–285. doi:10.1001/jamaophthalmol.2024.6113
7. Jiang X, Li Y, Chen N, Zhou M, He L. Corticosteroids for preventing postherpetic neuralgia. *Cochrane Database Syst Rev*. 2023;12(12):Cd005582. doi:10.1002/14651858.CD005582.pub5
8. Lee CN, Hsieh MH, Chen CY, Yang CC, Liao TC, Lai EC. Risk of herpes zoster and postherpetic neuralgia in patients with psoriasis treated with biologics: a nationwide study using a target trial emulation framework. *Br J Dermatol*. 2025;193(1):105–114. doi:10.1093/bjd/ljaf101
9. Li HL, Gong G, Wang JL, Li FB. Analysis of risk factors for postherpetic neuralgia in patients with postmalignancy herpes zoster. *Pain Physician*. 2023;26(4):E397–E403. doi:10.36076/ppj.2023.26.E397
10. Lin Z, Yu LY, Pan SY, Cao Y, Lin P. Development of a prediction model and corresponding scoring table for postherpetic neuralgia using six machine learning algorithms: a retrospective study. *Pain Ther*. 2024;13(4):883–907. doi:10.1007/s40122-024-00612-7
11. Wang C, Song X, Liu J, Song Y, Gao J. Analysis of risk factors and development and validation of a dynamic nomogram for postherpetic neuralgia: a retrospective study. *J Pain Res*. 2024;17:3935–3948. doi:10.2147/JPR.S483531
12. Liu L, Chen S. Construction of influencing factors and nomogram prediction model for post-herpetic neuralgia based on T cell function and inflammatory factors. *Front Med*. 2025;12:1619157. doi:10.3389/fmed.2025.1619157
13. Zhang L, Qu N, Li T, Duan L, Cui L. A scoping review of models for predicting the risk of postherpetic neuralgia. *Front Med*. 2025;12:1653680. doi:10.3389/fmed.2025.1653680
14. Ahmad KA, Shoaib RM, Ahsan MZ, et al. Microglial IL-10 and beta-endorphin expression mediates gabapentinoids antineuropathic pain. *Brain Behav Immun*. 2021;95:344–361. doi:10.1016/j.bbi.2021.04.007

15. Goins A, Patel K, Alles SRA. The gabapentinoid drugs and their abuse potential. *Pharmacol Ther*. 2021;227:107926. doi:10.1016/j.pharmthera.2021.107926
16. Iasonos A, Schrag D, Raj GV, Panageas KS. How to build and interpret a nomogram for cancer prognosis. *J Clin Oncol*. 2008;26(8):1364–1370. doi:10.1200/JCO.2007.12.9791
17. Lam N, Angel JC, Buchholz BA, et al. Asynchronous aging and turnover of human circulating and tissue-resident memory T cells across sites. *Immunity*. 2025;58(9):2271–2288.e2276. doi:10.1016/j.immuni.2025.07.001
18. Palacios-Pedrero M, Osterhaus A, Becker T, Elbahesh H, Rimmelzwaan GF, Saletti G. Aging and options to halt declining immunity to virus infections. *Front Immunol*. 2021;12:681449. doi:10.3389/fimmu.2021.681449
19. Peng Q, Guo X, Luo Y, et al. Dynamic immune landscape and VZV-specific T cell responses in patients with herpes zoster and postherpetic neuralgia. *Front Immunol*. 2022;13:887892. doi:10.3389/fimmu.2022.887892
20. Fetell M, Sendel M, Li T, et al. Cutaneous nerve fiber and peripheral Nav1.7 assessment in a large cohort of patients with postherpetic neuralgia. *Pain*. 2023;164(11):2435–2446. doi:10.1097/j.pain.0000000000002950
21. Oskay T, Keskin C, Özen M. Antioxidant and inflammatory biomarkers in herpes zoster. *J Med Virol*. 2022;94(8):3924–3929. doi:10.1002/jmv.27781
22. Liu J, Wang C, Li X, et al. Analysis of factors selectively related to herpes zoster involving peripheral sensory ganglia: retrospective study. *J Med Virol*. 2024;96(8):e29821. doi:10.1002/jmv.29821
23. Warner BE, Yee MB, Zhang M, et al. Varicella-zoster virus early infection but not complete replication is required for the induction of chronic hypersensitivity in rat models of postherpetic neuralgia. *PLoS Pathog*. 2021;17(7):e1009689. doi:10.1371/journal.ppat.1009689
24. Jiang D, Zhang Z, Ren F, Sun W. S100A8/A9 in herpes zoster neuralgia: molecular mechanisms and therapeutic perspectives. *Front Immunol*. 2025;16:1615638. doi:10.3389/fimmu.2025.1615638
25. Liang X, Fan Y. Bidirectional two-sample Mendelian randomization analysis reveals a causal effect of interleukin-18 levels on postherpetic neuralgia risk. *Front Immunol*. 2023;14:1183378. doi:10.3389/fimmu.2023.1183378
26. Ou M, Chen J, Yang S, Xiao L, Xiong D, Wu S. Rodent models of postherpetic neuralgia: how far have we reached? *Front Immunol*. 2023;14:1026269. doi:10.3389/fimmu.2023.1026269
27. Chen K, Wei X, Zhang W, Wang R, Wang Y, Yang L. Bone morphogenetic protein 4 derived from the cerebrospinal fluid in patients with postherpetic neuralgia induces allodynia via the crosstalk between microglia and astrocyte. *Brain Behav Immun*. 2024;119:836–850. doi:10.1016/j.bbi.2024.05.007
28. Kong C, Du J, Bu H, Huang C, Xu F, Ren H. LncRNA KCNA2-AS regulates spinal astrocyte activation through STAT3 to affect postherpetic neuralgia. *Mol Med*. 2020;26(1):113. doi:10.1186/s10020-020-00232-9
29. Wong C, Barkai O, Wang F, et al. mTORC2 mediates structural plasticity in distal nociceptive endings that contributes to pain hypersensitivity following inflammation. *J Clin Invest*. 2022;132(15). doi:10.1172/JCI152635
30. Fattori V, Zaninelli TH, Rasquel-Oliveira FS, et al. Nociceptor-to-macrophage communication through CGRP/RAMP1 signaling drives endometriosis-associated pain and lesion growth in mice. *Sci Transl Med*. 2024;16(772):eadk8230. doi:10.1126/scitranslmed.adk8230
31. Wang S, Jiang C, Cao K, Li R, Gao Z, Wang Y. HK2 in microglia and macrophages contribute to the development of neuropathic pain. *Glia*. 2024;72(2):396–410. doi:10.1002/glia.24482
32. Merriwether EN, Agalave NM, Dailey DL, et al. IL-5 mediates monocyte phenotype and pain outcomes in fibromyalgia. *Pain*. 2021;162(5):1468–1482. doi:10.1097/j.pain.0000000000002089
33. Vijayarajan SAL, Krolick KN, Quayle K, et al. Potential role for immune cell signatures as predictors of acute and chronic pain in adolescents post major musculoskeletal surgery. *Brain Behav Immun*. 2025;131:106133. doi:10.1016/j.bbi.2025.106133